Modeling of Linear Objects Considering Bend, Twist, and Extensional Deformations

Hidefumi Wakamatsu, Shinichi Hirai, and Kazuaki Iwata

Dept. of Mechanical Engineering for Computer-Controlled Machinery,
Osaka University, Suita, Osaka 565, Japan

Abstract

A systematic approach to the modeling of deformable fine linear objects is presented. Various deformable objects are manipulated in many manufacturing processes. Deformation of these objects is often utilized in order to manipulate them successfully while the manipulation sometimes fails because of unexpected deformation of the objects. Modeling of deformable objects is thus required so that the shape of the objects can be evaluated on a computer in advance.

In this paper, we will develop an analytical method to model the shape of a deformable linear object such as cords and tubes. First, a geometric representation to describe the shape of a linear object with bending and torsional deformation is introduced. The potential energy of the object and the geometric constraints imposed on it are then formulated. The shape of the object in the stable state can be derived by minimizing the potential energy under the geometric constraints. Next, procedure to compute the deformed shape is developed by applying a nonlinear programming technique. Finally, some numerical examples are shown in order to demonstrate how deformed shapes of linear objects are computed using the proposed approach.

1 Introduction

Many manufacturing processes that deal with deformable objects such as rubber tubes, sheet metals, cords, leather products, and paper sheets have been automated but handling and manipulative processes are still done by humans. Automatic handling and manipulation of deformable objects are thus eagerly required. Manipulative operations for deformable objects are often performed by utilizing their deformation actively while the operations may result in failure because of unexpected deformation of the objects during the manipulation process. Modeling of deformable objects is thus necessary so that we can evaluate the shape deformation of deformable objects on a computer in advance and can derive task strategies that carry out manipulative operations successfully.

In the past decades, solid modeling techniques have been developed in design and manufacturing area. Solid modeling systems have a capability of handling the shape of a rigid object on a computer and many design and manufacturing processes have been automated by use of modeling systems [1]. In the studies on rigid object manipulation, solid modeling techniques have been applied as well so that the model of the manipulated objects can be built. Thanks to the solid modeling techniques, a systematic approach to the manipulation of rigid objects has been developed recently. On the contrary, we have no systematic method of modeling deformable objects during their manipulative operations. Solid mechanics has been studied for a long time in order to analyze deformation of a solid body by investigating the relationship between stress and strain of the object [2]. It is not easy to analyze large deformation of a soft object such as paper and leather by solid mechanics approach, which basically deals with small deformation of a solid body. In computer graphics area, shape modeling of cloth objects has been proposed [3], and deformation of elastic objects has been studied [4]. These studies are not applicable to manipulative operations of deformable objects directly, since manipulation processes are not investigated in these studies.

In this paper, we will develop a systematic approach to the modeling of deformable linear objects such as cords and tubes. Firstly, the geometric representation of large deformation of a linear object in 3-dimensional space is established. Secondly, the potential energy of a linear object and the geometric constraints imposed on it are formulated so as to obtain the stable shape of the object based on the formulation. Thirdly, a procedure to compute the deformed shapes of a linear object is developed by applying a nonlinear programming technique. Finally, some numerical examples are shown in order to demonstrate how the proposed approach computes the deformation of linear objects.

2 Formulation of Deformation of Linear Objects

2.1 Geometric Representation of Deformed Linear Objects

In this section, we will formulate the geometrical shape of a linear object in three-dimensional space. Let L be the length of the object and s be the distance from one end point of the object along it. In order to describe the bend deformation of a linear object, we will introduce the global space coordinate system and the local object coordinate systems at individual points on the object, as shown in Figure 1. Let $O-xyz$

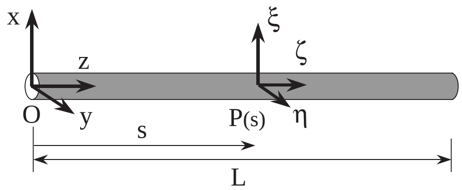

(a) natural shape

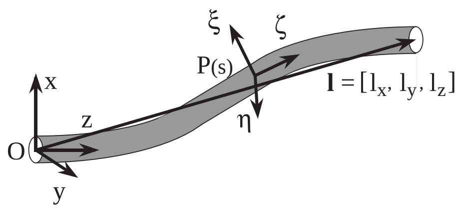

(b) deformed shape

Figure 1: Coordinates systems describing object deformation

be the coordinate system fixed on space and $P - \xi\eta\zeta$ be the coordinate system fixed on an arbitrary point $P(s)$ of the object. Select the direction of coordinates so that the ξ-axis, η-axis, and ζ-axis are parallel to x-axis, y-axis, and z-axis, respectively, in natural state where the object has no deformation. Bend deformation of the object is then represented by the relationship between the local coordinate system $P - \xi\eta\zeta$ at each point on the object and the global coordinate system $O - xyz$. Let us describe the orientation of the local coordinate system with respect to the space coordinate system by use of Eulerian angles, $\phi(s)$, $\theta(s)$, and $\psi(s)$. Namely, rotational transformation from coordinate system $P - \xi\eta\zeta$ to coordinate system $O - xyz$ is expressed by the following rotational matrix:

$$\begin{bmatrix} \mathrm{C}_\theta \mathrm{C}_\phi \mathrm{C}_\psi - \mathrm{S}_\phi \mathrm{S}_\psi & \mathrm{C}_\theta \mathrm{S}_\phi \mathrm{C}_\psi + \mathrm{C}_\phi \mathrm{S}_\psi & -\mathrm{S}_\theta \mathrm{C}_\psi \\ -\mathrm{C}_\theta \mathrm{C}_\phi \mathrm{S}_\psi - \mathrm{S}_\phi \mathrm{C}_\psi & -\mathrm{C}_\theta \mathrm{S}_\phi \mathrm{S}_\psi + \mathrm{C}_\phi \mathrm{C}_\psi & \mathrm{S}_\theta \mathrm{S}_\psi \\ \mathrm{S}_\theta \mathrm{C}_\phi & \mathrm{S}_\theta \mathrm{S}_\phi & \mathrm{C}_\theta \end{bmatrix}$$

For the sake of simplicity, $\cos\theta$ and $\sin\theta$ are abbreviated as C_θ and S_θ, respectively. Note that the Eulerian angles depend upon parameter s.

Let us describe the curvature of the object and its tortional angle, which are originated from differential geometry [5], in order to express bend and twist deformation of the object. Let κ and ω be the curvature and the tortional angle at point $P(s)$, respectively. It is found that the curvature and the tortional angle can be described by use of Eulerian angles ϕ, θ, and ψ as follows:

$$\begin{aligned} \kappa^2 &= \left(\frac{d\theta}{ds}\right)^2 + \sin^2\theta \left(\frac{d\phi}{ds}\right)^2 \\ \omega^2 &= \left(\frac{d\phi}{ds}\cos\theta + \frac{d\psi}{ds}\right)^2 . \end{aligned} \tag{1}$$

Note that the curvature κ and the tortional angle ω both depend on parameter s.

In order to express the extensional deformation of a linear object, we will introduce strains at each point $P(s)$. Let ε be extensional strain at point $P(s)$ on a linear object along its central axis. It turns out that a unit vector along ζ-axis at the natural state are transformed into the following vector due to the object deformation:

$$\begin{bmatrix} \zeta_x(s) \\ \zeta_y(s) \\ \zeta_z(s) \end{bmatrix} = (1 - \varepsilon) \begin{bmatrix} \sin\theta\cos\phi \\ \sin\theta\sin\phi \\ \cos\theta \end{bmatrix} \tag{2}$$

Let $x(s)$, $y(s)$, and $z(s)$ be spatial coordinates corresponding to point $P(s)$ along x-, y-, and z-axis, respectively. The spatial coordinates can be computed by integrating the above vector. Namely,

$$\begin{bmatrix} x(s) \\ y(s) \\ z(s) \end{bmatrix} = \int_0^s \begin{bmatrix} \zeta_x(s) \\ \zeta_y(s) \\ \zeta_z(s) \end{bmatrix} ds + \begin{bmatrix} x(0) \\ y(0) \\ z(0) \end{bmatrix} \tag{3}$$

where x_0, y_0, and z_0 denote $x-$, $y-$, and $z-$ coordinates at the end point corresponding to $s = 0$, respectively.

From the above discussion, we find that the geometrical shape of a deformed linear object can be represented by four variables, that is, Eulerian angles ϕ, θ, and ψ as well as extensional strain ε. Note that each variable depends upon parameter s.

2.2 Potential Energy and Geometric Constraints

In this paper, we will adopt a basic principle that the potential energy of a deformable object reaches to its minimum under the constraints imposed on it at its stable deformed shape. Dynamical effects during operations is assumed to be negligible. In this section, we will formulate the potential energy of a deformed linear object and geometric constraints imposed on the object.

Let us formulate the potential energy of a linear object. Assume that the thickness and the width of the object is negligibly small. Applying Bernoulli and Navier's assumption, it turns out that the potential energy U is described as follows:

$$U = U_{flex} + U_{tor} + U_{ext} + U_{grav} \tag{4}$$

where U_{flex}, U_{tor}, and U_{ext} represent flexural energy, tortional energy, and extensional energy of the object, respectively, and U_{grav} denotes its gravitational energy.

Flexural energy U_{flex} and tortional energy U_{tor} of the object can be computed by integrating flexural energy and tortional energy at point $P(s)$ over the object. Assuming that the flexural energy and the tortional energy are proportional to bending moment and twisting moment at each point $P(s)$, respectively, it turns out that they are described as follows:

$$\begin{aligned} U_{flex} &= \frac{1}{2}\int_0^L R_f \kappa^2 ds \\ U_{tor} &= \frac{1}{2}\int_0^L R_t \omega^2 ds \end{aligned}$$

where R_f and R_t represent the flexural rigidity and the tortional rigidity at point $P(s)$, respectively. Note that R_f and R_t may vary with respect to variable s. Assuming that the extensional energy is proportional to the extensional strain at each point $P(s)$, extensional energy U_{ext} is given as follows:

$$U_{ext} = \frac{1}{2}\int_0^L R_e \varepsilon^2 ds$$

where R_e denotes the extensional rigidity of the object, which may depends upon variable s. The gravitational energy is given by

$$U_{grav} = \int_0^L Dx ds$$

where D represents weight per unit length of the object. Quantity D may also vary with respect to parameter s.

Due to the interaction between a linear object and other objects such as fingertips and obstacles, some geometric constraints are imposed on the object. Let us derive the geometric constraints imposed on the object. The relative position between some points on the object is often controlled during object operations. Consider a constraint that specifies the positional relationship between two points on the object. Let $\boldsymbol{l} = [l_x, l_y, l_z]^T$ be a predetermined vector describing the relative position between two operational points, $P(s_a)$ and $P(s_b)$. Recall that the spatial coordinates corresponding to parameter s is given by eq.(3). Thus, the following equational condition must be satisfied:

$$\begin{bmatrix} x(s_b) \\ y(s_b) \\ z(s_b) \end{bmatrix} - \begin{bmatrix} x(s_a) \\ y(s_a) \\ z(s_a) \end{bmatrix} = \begin{bmatrix} l_x \\ l_y \\ l_z \end{bmatrix} \tag{5}$$

The orientation at some points of the object must be also controlled during the operation. These orientational constraints are simply described as follows:

$$\begin{array}{l} \phi(s_c) = \phi_c \\ \theta(s_c) = \theta_c \\ \psi(s_c) = \psi_c \end{array} \tag{6}$$

where ϕ_c, θ_c, and ψ_c are predefined angles at one operational point $P(s_c)$.

Contact between a linear object and rigid obstacles in operation space also yields other geometric constraints. Note that any points on the object must be located outside each obstacle or on it. Let us describe the surface of an obstacle fixed on space by function $h(x, y, z) = 0$. Assume that value of the function is positive inside the obstacle and is negative outside it. The condition that a linear object is not interfered with this obstacle is then described as follows:

$$h(x(s), y(s), z(s)) \leq 0, \quad \forall s \in [0, L] \tag{7}$$

where $x(s)$, $y(s)$, and $z(s)$ are described in eq.(3). Note that condition that an object is not interfered with obstacles is described by a set of inequalities, since mechanical contacts between the objects constraints the object motion unidirectionally.

From the above discussion, we find that the geometric constraints imposed on a linear object is given by not only equational conditions such as eqs.(5) and (6) but also inequality conditions such as eq.(7). The deformed shape of the object is, therefore, determined by minimizing potential energy described in eq.(4) under these geometric constraints imposed on the object. Namely, computation of the shape of a deformed object results in a variational problem under equational and inequality conditions.

3 Procedure to Compute Shapes of Deformed Linear Objects

Computation of the deformed shape of a linear object results in a variational problem as mentioned in the previous section. One method to solve a variational problem is Euler's approach, which is based on the stationary condition in function space. Recall that the geometric constraints resulting from mechanical contacts are unidirectional and are mathematically described by inequalities such as eq.(7). These conditions are nonholonomic constraints [6]. Thus, the shape of an object that minimizes potential energy does not necessarily satisfy the stationary condition. This implies that Euler's approach, which is based on the stationary condition, is not applicable.

In this paper, we will develop a direct method based on Ritz's method [7] and a nonlinear programming technique. Let us express functions $\phi(s)$, $\theta(s)$, $\psi(s)$, and $\varepsilon(s)$ by linear combinations of basic functions $\varphi_1(s)$ through $\varphi_n(s)$:

$$\begin{aligned} \phi(s) &= \sum_{i=1}^n a_i \varphi_i(s) \stackrel{\triangle}{=} \boldsymbol{a}^T \boldsymbol{\varphi}(s) \\ \theta(s) &= \sum_{i=1}^n b_i \varphi_i(s) \stackrel{\triangle}{=} \boldsymbol{b}^T \boldsymbol{\varphi}(s) \\ \psi(s) &= \sum_{i=1}^n c_i \varphi_i(s) \stackrel{\triangle}{=} \boldsymbol{c}^T \boldsymbol{\varphi}(s) \\ \varepsilon(s) &= \sum_{i=1}^n d_i \varphi_i(s) \stackrel{\triangle}{=} \boldsymbol{d}^T \boldsymbol{\varphi}(s) \end{aligned} \tag{8}$$

where $\boldsymbol{a}$, $\boldsymbol{b}$, $\boldsymbol{c}$, and $\boldsymbol{d}$ are vectors consisting of coefficients corresponding to functions $\phi(s)$, $\theta(s)$, $\psi(s)$, and $\varepsilon(s)$, respectively, and vector $\boldsymbol{\varphi}(s)$ is composed of basic functions $\varphi_1(s)$ through $\varphi_n(s)$. Substituting eq.(8) into eq.(4), potential energy U is described by a function of coefficient vectors; $\boldsymbol{a}$, $\boldsymbol{b}$, $\boldsymbol{c}$, and $\boldsymbol{d}$. The geometric constraints are also described by conditions involving the coefficient vectors. In addition, discretizing eq.(7) by dividing interval $[0, L]$ into N small intervals yields a finite number of conditions. As a result, a set of the geometric constraints is expressed by equations and inequalities with respect to the coefficient vectors.

The deformed shape of a linear object can be then derived by computing coefficient vectors $\boldsymbol{a}$, $\boldsymbol{b}$, $\boldsymbol{c}$, and

$\boldsymbol{d}$ that minimizes the potential energy under the geometric constraints. This minimization problem under equality and inequality conditions can be solved by use of a nonlinear programming technique such as multiplier method [8]. The deformed shape of the object corresponding to a set of coefficient vectors can be computed by use of eq.(3).

4 Numerical Examples

In this section, some numerical examples are shown in order to demonstrate how the proposed method computes the deformed shape of a linear object. The first example shows the shapes of a linear object topologically different each other. The second example demonstrates the effect of the extension of a linear object to its shapes. The third example shows the transition between topologically different shapes of a linear object. The following set of basic functions are used in the computation of these examples:

$$\varphi_1 = 1, \qquad \varphi_2 = s,$$
$$\varphi_{2n+1} = \sin \frac{2n\pi s}{L},$$
$$\varphi_{2n+2} = \cos \frac{2n\pi s}{L}. \qquad (n = 1, 2, 3, 4)$$

Assume that the length of the object L is equal to 100 in the following examples. In the nonlinear optimization for the computation of deformed shapes, multiplier method and simplex method are applied.

Topologically Different Shapes The first example shows topologically different shapes of a linear object. In this example, we assume that a linear object has no extension nor tortional strain at any point of the object and that its gravitational energy is negligible. Namely, potential energy consists of flexural energy alone; $U = U_{flex}$. In this case, it is found that extensional strain ε is equal to zero and that angles ϕ and ψ are constant. This implies that the linear object is deformed in a plane including z-axis. The tangential direction at both endpoints is assumed to coincide with the z-axis, that is, angles $\theta(0)$ and $\theta(L)$ are equal to zero or multiple of 2π. Without loss of generality, we can assume that angle $\theta(0)$ is equal to zero. Let relative distance l_x and l_y between the two endpoints of the object along x-axis and y-axis be both equal to zero. Suppose that there exists a rigid obstacle defined by equation $x \leq 0$. Individual points of the linear object thus must satisfy this inequality. Figure 2 illustrates the computational results of deformed shapes under the above constraints with respect to some values of relative distance l_z between the endpoints along z-axis; $0.6L$, $0.4L$, $0.2L$, where L denotes the length of the object. Figure 2-(a) shows the deformed shapes in the case that angle $\theta(L)$ is equal to zero. The shapes corresponding to the figure have no knots. These are referred to as *mode 1* shapes of a linear object in this article. Figure 2-(b) describes the deformation where $\theta(L)$ is equal to 2π and we find that the individual shapes corresponding to the figure include one knot. These are referred to as *mode 2* shapes of the object.

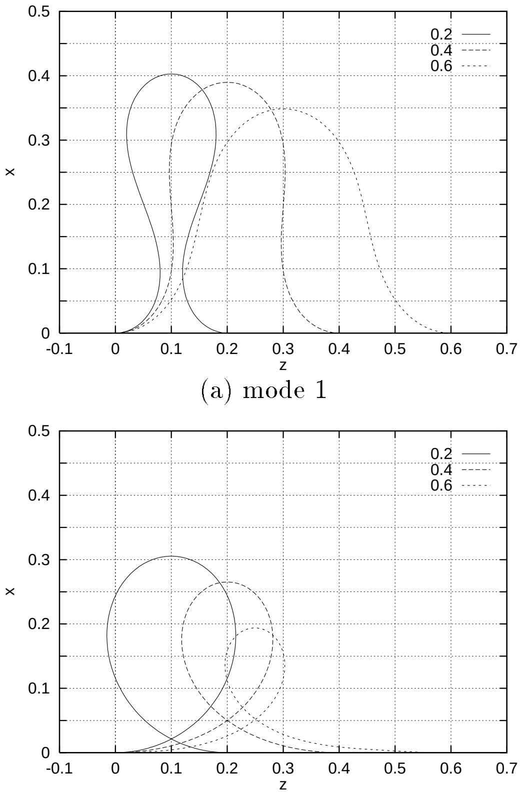

(a) mode 1

(b) mode 2

Figure 2: Example of computed object shapes

Since the number of knots differs, the object shape of mode 1 and that of mode 2 are topologically different each other. Thus, it turns out that the proposed method has a capability of computing topologically different shapes of a linear object with large deformation, as shown in the figure.

Figure 3 shows the computed potential energy corresponding to both modes of a linear object. The transverse axis denotes the distance between the endpoints along z-axis relative to the object length L, that is, l_z/L. Recall that the potential energy of a deformable object reaches to its minimum at its stable deformed shape. Thus, a linear object can have topologically different shapes during one process when the rotation around the central axis of the object is allowed at one endpoint. In this case, we find that a linear object has the shape of mode 1 when the distance between the endpoints is large while the shape is of mode 2 when the distance is small and the object is deformed significantly. Note that the object shape transits between mode 1 and mode 2 once the relative distance becomes about 0.42, where the two energy curves in the figure intersect.

Effect of Object Extension The second example demonstrates the computation of the object shape considering the extensional energy. Namely, potential energy of a linear object is given by the sum of the flex-

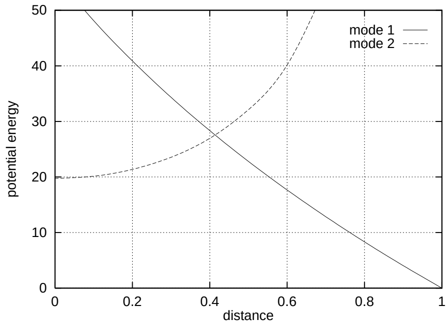

Figure 3: Potential energy

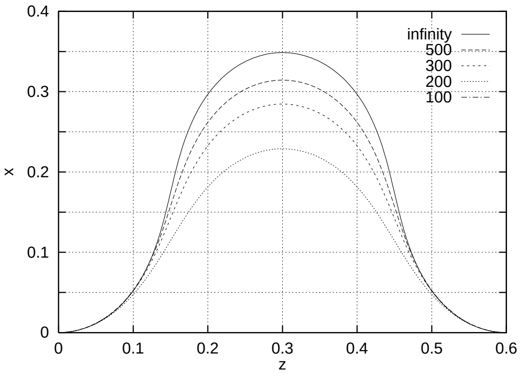

Figure 4: Example of computed object shapes considering extension

ural energy of the object and its extensional energy; $U = U_{flex} + U_{ext}$. Normalizing the potential energy and the geometric constraints by dividing variable s by length L, we find that the shape of the object is determined by the following dimensionless quantity:

$$\rho = \frac{R_e}{R_f} L^2.$$

Quantity ρ represents the contribution of the extensional energy to the shape of a linear object. The object has less extension for the larger quantity ρ. Especially, the object has no extension at $\rho = \infty$. Let us compute the deformed shapes of a linear object of length L corresponding to various values of ρ; ∞, 500, 300, 200, and 100. The distance between the endpoints along z-axis is given by $0.6L$ in this computation. These shapes are shown in Figure 4. Note that the object is reduced and the length of the object is less than the original length L. The height of the object go down and the length of the object is more reduced with decreasing quantity ρ, as shown in the figure. Extremely, extensional deformation alone is caused and no flexural deformation of the object occurs when parameter ρ exceeds 100.

Object Shapes Considering Bending and Torsion The third example demonstrates the deformed shapes of a linear object computed by considering its bending and tortion. Namely, potential energy of the object is assumed to be given by the sum of flexural energy and tortional energy of the object; $U = U_{flex} + U_{tor}$. Let us reduce a linear object of its length L along the central axis of the object. Suppose that Eulerian angles at both endpoints are equal to zero, that is, the following constraints are imposed on the object; $\phi(0) = \phi(L) = 0$, $\theta(0) = \theta(L) = 0$, and $\psi(0) = \psi(L) = 0$. Assume that dimensionless quantity R_f/R_t, which determines the object shape, is equal to 100. Let us show the computed shapes corresponding to various values of the distance between two endpoints; $0.8L$, $0.7L$, $0.6L$, $0.5L$, $0.4L$, and $0.3L$. Computed shapes of the object are shown in Figure 5. Since the object shape is not planar for some values of the distance, the top view, the front view, and the side view are shown in the figure. The shape of the object is involved in x-z plane and is of mode 1 when the distance is equal to $0.8L$ or $0.7L$. The object is twisted and is not involved in any plane when the distance is equal to $0.6L$ or $0.5L$. The object contains one knot, that is, it has a shape of mode 2 when the distance is equal to $0.4L$ or $0.3L$. Thus, It turns out that the object shape transits from mode 1 into mode 2 as the distance between the endpoints decreases. Recall that the direction of the central axis of the object and the orientation around the axis are fixed at both endpoints due to the geometric constraints imposed on the object. This implies that the linear object must have a non-planar shape during the transition between mode 1 and mode 2, as illustrated in Figure 6-(a) through Figure 6-(d).

Since we use trigonometric functions as basic functions, local sharp bendings cannot be computed well. It is expected to select another set of basic functions in order to cope with sharp bendings.

5 Concluding Remarks

An analytical approach to the modeling of deformable linear objects has been developed based on the physical properties of the objects. Firstly, the geometric representation of a linear object with large flexural, torsional, and extensional deformation was established by use of differential geometry. It is found that the shape of a linear object can be described by Eulerian angles and extensional strain. Secondly, the potential energy of a linear object and the geometric constraints imposed on it were formulated. It turns out that not only equational constraints resulting from predefined condition on the object motion but inequality constrains resulting from unidirectional nature of mechanical contacts are imposed on the object. Stable deformed shapes of the object can be derived by minimizing the potential energy under the geometric constraints. Next, a procedure to compute the deformed shape of the object was developed by applying nonlinear programming technique. Some numerical examples proved that the procedure had a capability of computing the large deformation of a fine linear object.

Using the modeling technique proposed in this paper, we can evaluate the deformed shape of a linear

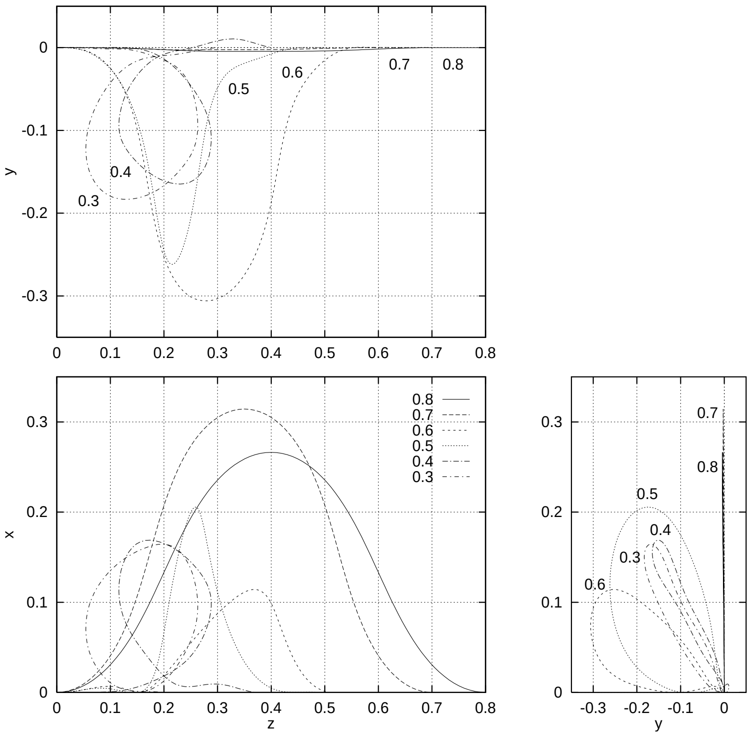

Figure 5: Example of computed object shapes considering bending and torsion

object in three-dimensional space under various conditions on a computer. It is expected that this approach enables us to plan manipulative operations that deal with deformable linear objects.

References

[1] Mäntylä, M., *An Introduction to Solid Modeling*, Computer Science Press, 1988

[2] Fung, Y. C., *Foundations of Solid Mechanics*, Prentice-Hall, 1965

[3] Weil, J., *The Synthesis of Cloth Objects*, Computer Graphics, Vol 20, No.4, pp.49-54, 1986

[4] Terzopoulos, D. et al., *Elastically Deformable Models*, Computer Graphics, Vol 21, No.4, pp.205-214, 1987

[5] Auslander, L., *Differential Geometry*, Harper International Edition, 1977

[6] Goldstein, H., *Classical Mechanics*, Addison-Wesley, 1980

[7] Elsgolc, L. E., *Calculus of Variations*, Pergamon Press, 1961

[8] Avriel, M., *Nonlinear Programming: Analysis and Methods*, Prentice-Hall, 1976

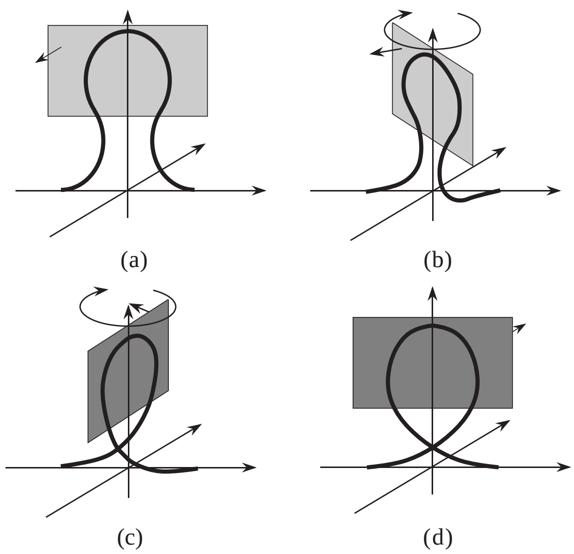

Figure 6: Transition between topologically different shapes